Surface chemical reaction of laser ablated aluminum sample for detonation initiation

Chang-hwan Kim, Ardian B. Gojani, and Jack J. Yoh*
School of Mechanical and Aerospace Engineering
Seoul National University, Seoul, Korea 151-742

1 Introduction

Laser ablation is the principle mechanism upon which many laser processing techniques rely, including materials processing, laser propulsion, and chemical analysis of materials of interest. Ablation of a solid material by a laser beam requires delicate control of working parameters that include focusing spot size, wavelength, pulse duration, and incident irradiance. An important factor on this account is the ambient condition since the ablation process in air may encounter strong laser supported waves [1].

Laser-supported combustion (LSC) waves and laser-supported detonation (LSD) waves in moderate irradiance regime (order of $10^8 - 10^{12} \mathrm{W/cm^2}$) have been the topics of numerous investigations, starting in mid 1960s with the works of Ramsden and Savic [2] and Raizer [3], with the aim to explore the complex non-linear heating phenomena that are usually present in laser beam-metal interactions involving plasma formation. More recently, LSD wave termination and conditions for its transition into LSC has been investigated [4]. Initial part of the energetic laser pulse vaporizes and ionizes the surface of a metal, forming a layer of rapidly expanding hot and dense plasma. This plasma absorbs the later part of the laser pulse, effectively shielding the metal surface from the incoming beam, thus initiating a series of waves that propagate away from the metal surface towards the laser beam. Most noticeably, the expanding plasma acts as a piston on the surrounding air, driving a shock wave. Upon laser pulse termination, these waves will continue propagating while dissipating their energy into the surrounding ambient.

In this paper, we consider the evolution of metal plasma generated by high laser irradiances ($\sim 10^{12} \mathrm{W/cm^2}$) and its effect on the surrounding air by using shadowgraph images at much later times after laser pulse termination; hence after the laser supported detonation and combustion processes have been completed. The essence of the paper is in observing initiation of chemical reactions between ablated aluminum plasma and oxygen from air by inducing high power laser pulse (>1000 mJ/pulse), and conduct a quantitative comparison of chemically reactive laser initiated waves with the classical detonation of exploding aluminum (dust) cloud in air, with the goal to provide a new method of initiating detonation from metal sample in air via the high power laser experiment.

To connect chemical process of laser initiated wave phenomena with the classical detonation, it is imperative to understand the aluminum particle combustion in open air. For the initiation and detonation of energetic powder in air, Zhang and Gerrard have experimentally determined detonability of fine aluminum particles suspended in air which relates the explosion limit of energetic metal

Correspondence to: jjyoh@snu.ac.kr

particle-gas flow [5]. Although both aluminum powder detonation and the surface chemical reaction induced by laser share the similarity in the resulting detonative behavior, the initiation methods differ. From [6] and [7], one can analytically determine the Chapman-Juguet (CJ)-limits and compare the resulting laser initiated detonation state. In the experiment, detonation wave is observed when focused laser energy was above 1000 mJ (up to 2500 mJ) per laser pulse. At these high pulse energy, experimental data are in agreement with available detonation velocity and pressure ratio of aluminum power from the literature. Moreover, to bolser our objective of providing strong evidence of surface reaction of aluminum sample, X-ray Diffraction (XRD) was used to examine the process of reaction in the aluminum cloud in air. This paper suggests a potential for igniting energetic metal substance in air via the high power laser, by using non-powder form of the metal sample.

2 Experimental setup

The experimental setup for visualizing the chemically reactive wave of aluminum in air is shown in Fig. 1. The laser used for target ablation is a Q-switched Nd:YAG laser (Continuum Powerlite Plus II of maximum 3 J/pulse) with 7 ns pulse duration at wavelength of 1064 nm. The light source for shadowgraph imaging was an Nd:YAG laser (Continuum Minilite) with 532nm wavelength and 3 ns pulse duration. This beam, which is aligned parallel to the aluminum target and perpendicular to the ablation laser beam, reaches the target in several nanoseconds after the ablation. By passing through concave and convex lenses, the beam is sufficiently collimated, and then is focused in the front of a CCD camera (Nikon D80) to give a focused shadowgraph. The luminosity of ablation plasma is high, therefore a neutral density filters is applied ahead of the camera sensor. This also necessitates the use of a laser light for visualization, because lasers can produce more luminous beams than the flash of the plasma. The synchronization of the experiment is done by a pulse generator (565-8CG, 100 MHz and 500 ps delay time), allowing both lasers to be triggered by a single delay generator. Timing of the lasers is also monitored by a fast oscilloscope (Tektronix TDS-2014) coupled with fast rise time photodiodes (~1 ns).

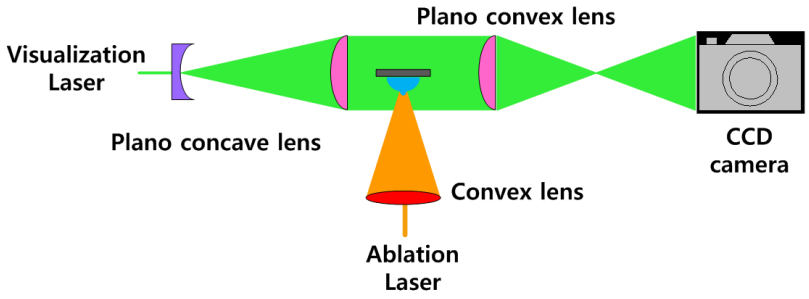

Figure1. Schematic of the standard shadowgraph imaging system

3 Results and discussion

Figure 2 shows the shadowgraph images of laser induced plasma of aluminum in air that are obtained at different time delays between ablation and visualization laser with different energies for the ablation laser. Since in our experimental setup the camera operates only in a single shot mode, each presented image is obtained from a fresh ablation. Nevertheless, the images testify for a highly reproducible phenomenon, which was also tested by carrying out at least 3 experiments under the same conditions. The shock and plasma fronts are clearly observed, due to very different electron densities of ambient air and plasma. By this shadowgraph technique, one can see not only the plasma and shock wave propagation but also the excited non-linear thermal waves within the shock wave [8]. This is because shadowgraph images allow the specific observation of the propagation of different compression states during the beam-matter interaction. Images at both laser energy regimes show some similar features, such as the external shock wave, the ionization front, and the heat waves at the

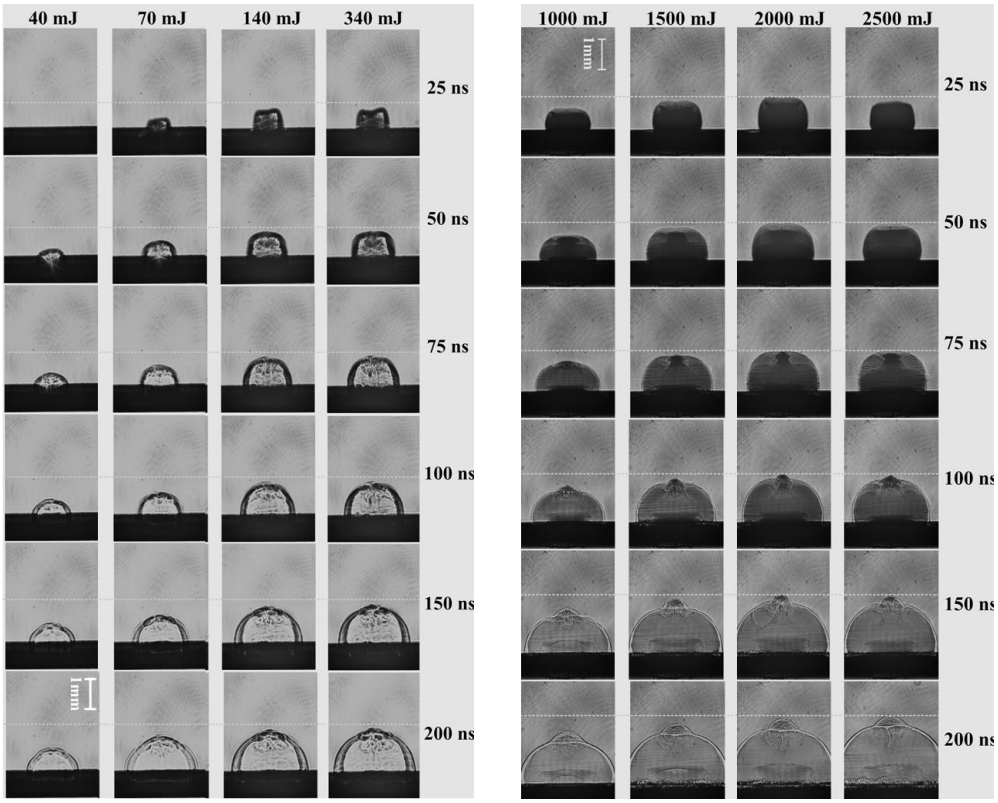

Figure2. Shadowgraph images at increasing delay times in 1 atm over an aluminum target

tip of the shock in axial direction. But, several differences are clearly observed. For example, the distance between the shock wave (the dark stripe) and the ionization front (the bright stripe) is very different. In the low energy case they are at a considerable distance from each other, while in the high energy case they are almost overlapping. The high energy case also results in a large amount of ablated material, primarily in liquid phase and ejected due to phase explosion [9]. This plume is visible in the shadowgraphs, contrary to the low energy case. This also enhances the visibility of internally propagating shock wave. It should be noted that the plume propagates a distance which is only a fraction of the distance covered by the shock wave. Since the laser energy is not enough to ablate aluminum target fully for 40 mJ to 340 mJ, the shock velocity increased continuously with increasing laser energy. When the energy is raised beyond 1000 mJ per pulse, one sees the detonation wave front ahead of a shock wave. Even if the laser energy is increased beyond 1500 mJ, the maximum velocity or CJ detonation velocity remained constant; the CJ detonation velocity of aluminum-air detonation is a material property, not a condition dependent quantity. In other words, by having highly ionized state condition, compressed aluminum vapors form while breaking bonding energy of oxygen for initiating chemical reaction.

Imaging technique allowed us to directly measure the wave velocities, as shown in Fig. 3, from which pressure, density, and temperature can be calculated by using the Rankine - Hugoniot condition [10]

$$p_s = \frac{\rho_o V_s^2}{\gamma_{metal} + 1} \qquad (2)$$

where p_s is the pressure of the detonation wave, V_s is the velocity of the detonation wave, γ_{metal} is the specific heat ratio of metal (Aluminum, 5/3), and ρ_o is the density of the ambient gas. For the first 25 ns, the plasma expanded with velocities equal to 15 x 10^3 m/s for the 70 mJ laser pulse, up to 36 x 10^3 m/s for 2500 mJ laser pulse. These very high velocities rapidly decrease to values of a few km/s.

From parallel spectroscopic measurements [11], temperature in the plasma region is determined to be on the order of 10^4 K. Since the ionization energy of aluminum is almost half the value of air, the overwhelming energy from the laser is spent in aluminum ionization, as opposed to air. Hence, main constituents of plasma are aluminum atoms and ions. It is measured [12] that laser irradiance comparable to those used in this study ablates a fraction of a milligram of material.

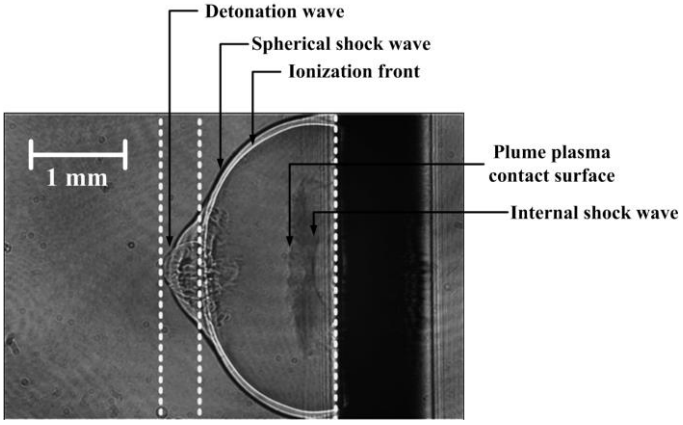

Figure3. The specific structure of LS wave

The speed of detonation wave is calculated by image resolution method which uses the ratio of the pixel to the real length. Before getting velocity, shock and detonation wave radius versus time data were obtained from the shadowgraph images. The line representing the fitted curve, and the data points are shown in Fig. 4 which is used for Deway fitting equation [13]. To obtain the detonation velocity, we calculated the speed of spherical shock wave and the leading point of a detonation wave. Then by subtracting leading point velocity from shock wave speed, we get detonation velocity. In the high irradiance regime ($\sim 10^{12}\,W/cm^2$), these velocities are 1591±90 m/s, 1672±25 m/s, 1714±90 m/s, and 1717±119 m/s for probing laser energies from 1000 to 2500 mJ, which are shown in Figs. 4 and 5. The error corresponds to the standard deviation of the mean from three measurements. As expected, the uncertainty is higher initially at about 6%, approximately 50 ns after laser ablation. Later, the determination of detonation velocity becomes more accurate, and the remainining source of error come from the uncertainty of imaging shock positions in a pixel. In our imaging setup, a pixel corresponds to 5 um, therefore the errors are smaller than a few percent. Calculations of pressure ratios based on Eq. (2) and the detonation velocities give the values for pressure ratios as 12.63±2.47, 13.87±0.71, 14.63±2.65, and 14.76±3.53.

At the low energy regime (40-340 mJ), typical laser ablation plume is seen to be without significant thermal excitation. The increase of laser energy causes the velocity of shock wave to rise as well. The highly ionized, excited aluminum vapor and compressed ambient gas (N_2, O_2 etc) in the front of a shock wave is observed only when laser energy was above 70 mJ. When the energy is raised beyond 1000 up to 2500 mJ per pulse, one can see the detonation wave front ahead of a shock wave. In this energy range, the increase of energy did not affect the velocity, indicating that the CJ detonation velocity has been achieved. In the case of shock tube explosion of aluminum dust in air, the aluminum detonation velocity is measured to lie in the range of 1300-1800 m/s [6, 7, and 14] which means that chemical reaction processes occur at stable reaction state, where the end states are characterized by its sonic states.

The factors that are accountable for the aluminum surface reaction upon laser ablation include the reaction product formation of Al2O3. Figure 6 clearly displays significant Al2O3 trace, fundamental to chemical reaction of aluminum with oxygen. The lines show the measured XRD features of aluminum sample that are compared to the joint committee on powder diffraction standards (JCPDS) powder diffraction dada. As presented, the detected aluminum oxide (Al2O3) indicates chemical reaction occurrance on the aluminum surface, which supports LS wave phenomena associated with the

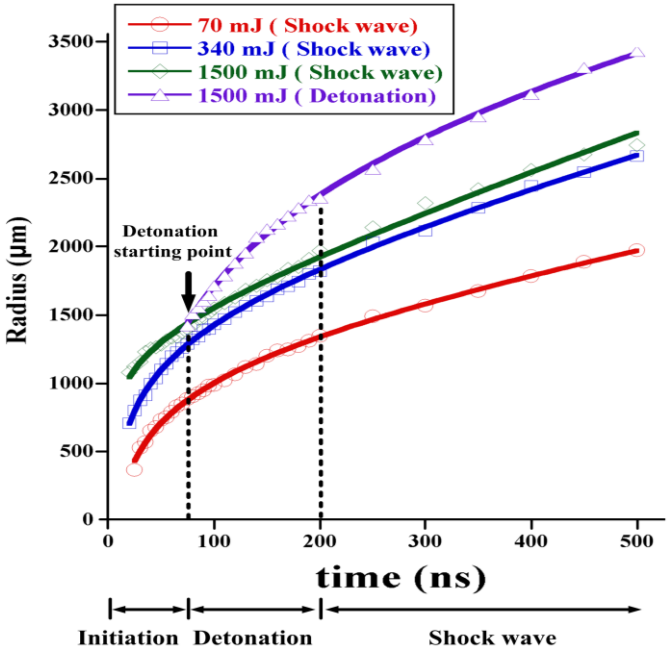

Figure4. Measured radius of propagation for different energy levels

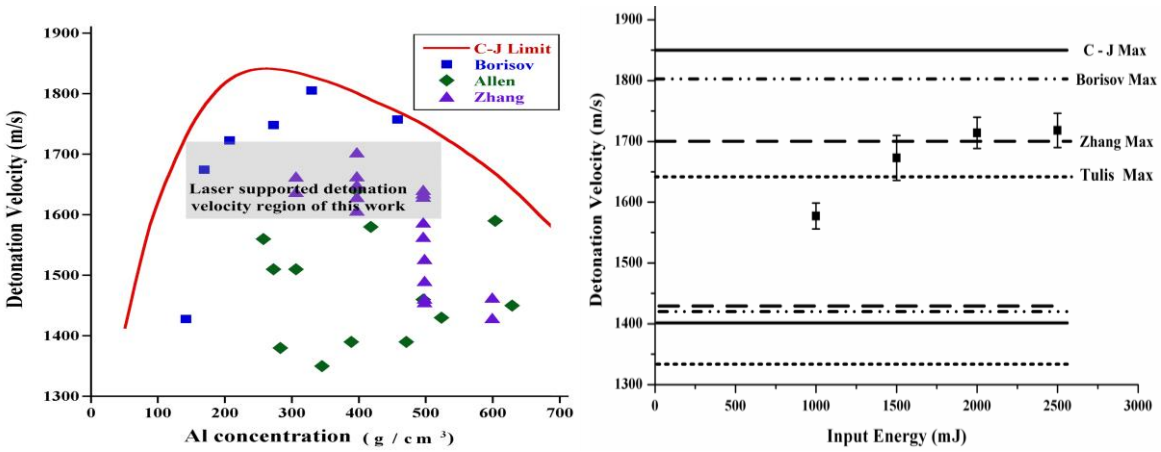

Figure5. Comparison between other detonation and quasi-detonation velocities and LS wave detonation velocity

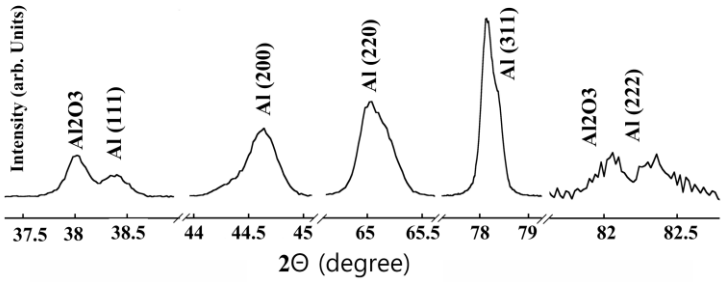

Figure 6. X-Ray Diffraction (XRD) of the aluminum plate deposited at room temperature and 1500mJ of laser energy

aluminum-oxygen chemical reaction. The supposed reaction mechanism is composed of four gas phase reactions, one heterogeneous reaction at the aluminum surface and one heterogeneous reaction at the surface of the aluminum oxide [15] that results in Al_2O_3 reaction product. With the velocity

analysis from shadowgraph measurement and the XRD measurement of the reaction product, it is probable that detonation of aluminum cloud lifted by the laser excitation in air has occured in the present test.

4 Conclusion

Experimental observations indicate that the chemically reacted aluminum sample in air via high irradiation ($10^{11}-10^{12}\,W/cm^2$) confirms the classical CJ detonation condition of aluminum-air combustion for detonation velocity, pressure ratio and XRD data. The present work establishes the laser initiation of detonation as it appears during the high power irradiation on an aluminum sample. Shadowgraph visualization enabled the structure of detonation waves that consists of the von Neumann peak (head shock) followed by the CJ reaction shock wave. At the low energy regime (40 - 340 mJ), the velocity of LS wave is increased when the energy of laser is raised, which means that a considerable part of the laser energy is absorbed at the target, resulting in increase of vaporized mass. On the higher energy range (1000 – 2500 mJ), chemical detonation waves appeared which follow velocity and pressure of the standard aluminum particles – air detonation. The process of initiating energetic metal sample in a bulk form as opposed to a powder is suggested in this work. Titanium and boron samples are being tested.

References

[1] Root RG. Modeling of post-breakdown phenomena. (1989). Laser-induced plasmas and applications. Marcel-Dekker. 69-103.
[2] Ramsden SA, Savic P. (1964). A radiative detonation model for the development of a laser-induced spark in air. Nature. 203 (4951): 1217-1219.
[3] Raizer Yu. P. (1965). Heating of a gas by a powerful light pulse. Soviet Physics JETP. 21:1009.
[4] Ushio M, Komurasaki K, Kawamura K, Arakawa Y. (2008). Effect of laser supported detonation wave confinement on termination conditions. Proceedings Shock Waves. 18(1): 35.
[5] Zhang F, Gerrard K, Ripley RC. (2009). Reaction mechanism of aluminum-particle-air detonation. Journal of Propulsion and Power. 25(4): 845-858.
[6] Tulis AJ, Selman JR. (1982). Detonation tube studies of aluminum particles dispersed in air. Proceedings of the 19th International Symposium on Combustion, Combustion Inst. 655–663.
[7] Zhang F, Murray SB, Gerrard K. (2006). Aluminum Particles-air Detonation at Elevated Pressures. Shock Waves. 15: 313.
[8] Grevel JFY, Boudreau D. (2009). Study by focused shadowgraphy of the effect of laser irradiance on laser-induced plasma formation and ablation rate in various gases. Spectrochimica Acta. Part B 64: 56.
[9] Wen SB, Mao X, Greif R, Russo RE. (2007). Expansion of the laser ablation vapor plume into a background gas. J. Appl. Phys, 101:023115.
[10] Zeldovich Ya. B, Raizer Yu. P. (2002). Physics of shock waves and high-temperature hydrodynamic phenomena. Dover. New York.
[11] Thorne A, Litzen U, Johanson S. (1999). Spectrophysics: Principles and Applications. Springer. Berlin. 2nd ed.
[12] Gojani AB, Yoh JJ. (2009). New ablation experiment aimed at metal expulsion at the hydrodynamic regime. Applied Surface Science. 255: 9268.
[13] Kleine H, Deway JM, Ohashi K, Mizukaki T, Takayama K. (2003). Studies of the TNT equivalence of silver azide charges. Shock waves. 13(2): 123-138.
[14] Borisov AA, Khasainov BA, Saneev EL, Formin IB, Khomik SV, Veyssiere B. (1991). Dynamic structure of detonation in gaseous and dispersed media. Kluwer Dordrecht. 215-253.
[15] Ogle RA, Beddow JK, Chen LD, Butler PB. (1988). An investigation of aluminum dust explosions. Combustion Science and Technology. 61: 75-99.